Sensitivity enhancement of WS_2-coated SPR-based optical fiber biosensor for detecting glucose concentration*

Yun Cai(蔡云)[1,4], Wei Li(李卫)[1,2,3,4,†], Ye Feng(冯烨)[1,4], Jian-Sheng Zhao(赵建胜)[1,4], Gang Bai(白刚)[1,4], Jie Xu(许杰)[1,4], and Jin-Ze Li(李金泽)[1,4]

[1] *College of Electronic and Optical Engineering & College of Microelectronics, Nanjing University of Posts and Telecommunications, Nanjing* 210023, *China*
[2] *State Key Laboratory of Millimeter Waves, Southeast University, Nanjing* 210093, *China*
[3] *State Key Laboratory of Luminescent Materials and Devices, South China University of Technology, Guangzhou* 510641, *China*
[4] *Research Center of Optical Communications Engineering & Technology, Nanjing* 210023, *China*

(Received 17 April 2020; revised manuscript received 8 July 2020; accepted manuscript online 15 July 2020)

In this paper, we propose a theoretical model of the surface plasmon resonance-based optical fiber biosensor for detecting glucose concentration. The Au/ZnO/WS_2 multilayer film is coated around optical fiber. Compared with the conventional surface plasmon resonance sensor, WS_2 material can increase the sensitivity of the biosensor. The absorption capacity of WS_2 is used to load glucose oxidase by forming a sensitive area to recognize glucose. Refractive index of the solution is calculated and then the concentration of the glucose can be obtained by the correspondence between refractive index and glucose concentration. The highest sensitivity of the SPR biosensor with a structure of 40-nm Au/5-nm ZnO/14 layers of WS_2 is 4310 nm/RIU. The proposed WS_2-based SPR fiber biosensor has a unique effect on the detection of glucose concentration. It is expected to have potential applications in future medical blood glucose concentration detection.

Keywords: surface plasmon resonance, optical fiber, biosensor, glucose

PACS: 07.07.Df **DOI:** 10.1088/1674-1056/aba601

1. Introduction

Diabetes is a common metabolic disease which is very harmful for people's health. Blood glucose detection is an important part of the diagnosis and treatment of diabetes clinically. An efficient, sensitive and reliable glucose concentration detection method is of great significance. Different methods of detecting glucose concentration have been applied to the existing researches, such as electrochemical, surface-enhanced fluorescence, and surface-enhanced Raman spectroscopy.[1] Recently, surface plasmon resonance (SPR) sensor with glucose oxidase (GOx) has proven that it can be another effective method. It has ability to isolate interference from other components which are found in blood because of the specificity and sensitivity to glucose concentration.[2–4] Conventional prism-based SPR sensors usually use angle modulation, which has some deficiencies like large size. It is not suitable for long-distance applications. Moreover, the oxidation of the metal and the poor biosorption capacity of metal surface limit the performance of the traditional SPR sensors.[5] Prism sensors are gradually replaced by optical fiber in some specific fields. Optical-fiber SPR sensors use wavelength modulation, which conduces to flexible optical design, strong anti-electromagnetic interference capability, remote sensing applications, and real-time dynamic monitoring.[6–8] For these reasons, the methods of metal nanoparticles,[9,10] nanopores,[11] and heterostructures[12] were proposed. Lahav *et al.*,[13] Shalabney and Abdulhalim[14] reported an increase of sensitivity by adding a high refractive index (RI) layer. The adding of materials is an excellent method , such as adding the transition metal oxides or graphene into the metallic film.[15,16] Also, two-dimensional nanomaterial has been greatly concerned due to its unique applications in biosensors.[17–19]

In recent years, GOx-based reagent-free biosensor for highly sensitive and effective detection of glucose has become a hot research spots.[20–26] Zhang *et al*. reported that GOx was detected by a novel glucose biosensor with gold nanoparticles–carbon nanotube composite film.[27] Usha *et al*. proposed that the biosensor structure of Ag/ZnO nanorods/GOx was able to detect the concentration of glucose by electrostatically adsorbing the GOx.[28] In the present paper, we propose a theoretical model of the surface plasmon resonance-based optical fiber biosensor for detecting glucose concentration. The Au/ZnO/WS_2 multilayer films are coated around optical fiber. WS_2, a kind of two-dimensional transition metal disulfide material, has become a key research material. It has been reported that the WS_2 has good application prospects in high sensitivity sensors and biomedical fields.[28–30] It is a graphene-like material with fullerene

*Project supported by the Natural Science Foundation of Jiangsu Province, China (Grant No. BK20171442), the China Postdoctoral Science Foundation (Grant No. 2018T110480), the Open Foundation of State Key Laboratory of Millimeter Waves, China (Grant No. K202003), the Open Foundation of State Key Laboratory of Luminescent Materials and Devices, China (Grant No. 2020-skllmd-03), and the Fund from the Research Center of Optical Communications Engineering & Technology, Jiangsu Province, China (Grant No. ZXF201904).

†Corresponding author. E-mail: Liw@njupt.edu.cn

© 2020 Chinese Physical Society and IOP Publishing Ltd

structure, excellent optical properties, moderate carrier mobility, and high density of the electronic states. Due to its two-dimensional structure with a high surface-to-volume ratio, WS_2 can enhance biocompatibility and act as a load.[31]

2. Design consideration and theoretical model

Figure 1 shows the schematic diagram of the structure of the sensing system. The fiber core is coated by Au/ZnO/WS_2/sensing multilayer film to form an SPR optical fiber sensor. The SPR sensing mechanism is based on the principle of attenuated total reflection with Kretschmann's configuration with wavelength interrogation mode.[32] When a certain wavelength of p-polarized light propagates in the fiber, total internal reflection occurs. Due to the peculiarity of p-polarized light, it is not reflected immediately but will enter into the Au film in the form of evanescent wave in the horizontal direction and continue to propagate. On the surface of the Au film, the free electrons are stimulated. Then, the surface plasmon waves which propagate along the interface are generated. Surface plasmon wave is exponentially decayed. Once the wave vector matches with the surface plasmon wave, the surface plasmon resonance occurs and the reflected light energy drops sharply. This resonance is observed as a sharp dip in the output spectrum. When the glucose solution flows through the sensor surface, the RI of glucose solution can be measured by fitting the SPR resonance wavelength and then further confirm the glucose concentration.

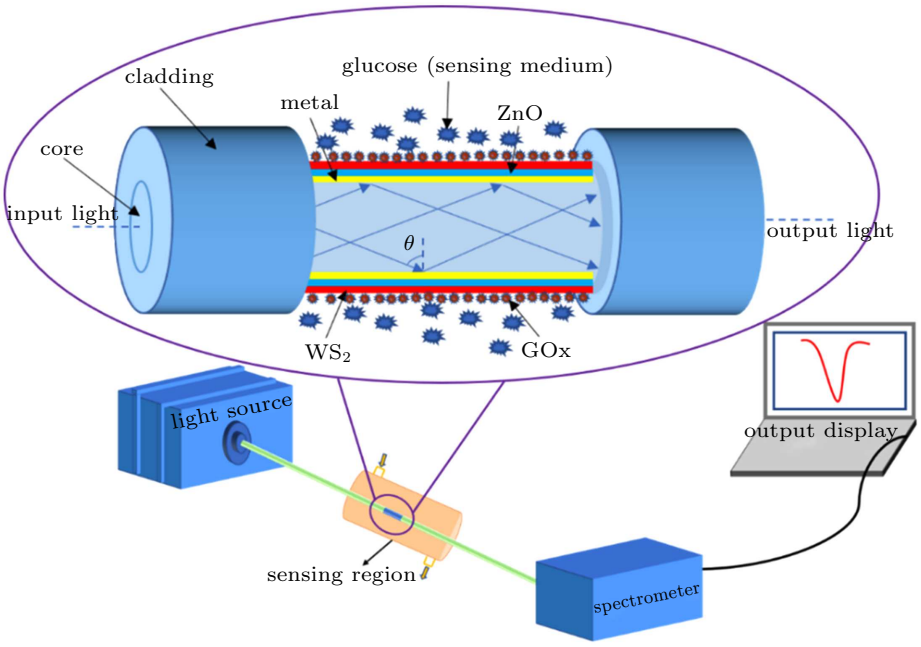


Fig. 1. Schematic diagram of SPR fiber biosensor.

The following dispersion determines the relationship between the RI of the fiber and the wavelength, and it is expressed as

$$n_1(\lambda) = \sqrt{1 + \frac{A_1\lambda^2}{\lambda^2 - B_1^2} + \frac{A_2\lambda^2}{\lambda^2 - B_2^2} + \frac{A_3\lambda^2}{\lambda^2 - B_3^2}}, \tag{1}$$

where λ is the wavelength, A_1, A_2, A_3, B_1, B_2, and B_3 are coefficients.[33]

The dielectric constant of Au is determined by the Drude model as follows:

$$\varepsilon_m(\lambda) = 1 - \frac{\lambda^2\lambda_c}{\lambda_p^2(\lambda_c + i\lambda)}, \tag{2}$$

where λ_p and λ_c are the plasma and the collision wavelength, respectively. For Au, $\lambda_p = 1.6826\times10^{-7}$ m and $\lambda_c = 8.9342\times10^{-6}$ m.[34]

The dielectric function of ZnO is defined as follows:

$$\varepsilon(\omega) = \varepsilon_\infty - \frac{\omega_p^2}{\omega^2 + \gamma^2} + i\frac{\gamma\omega_p^2}{\omega(\omega^2 + \gamma^2)}, \tag{3}$$

where ε_∞, ω_p, and γ are the high frequency dielectric constant, the plasma frequency, and the damping frequency. Here, $\varepsilon_\infty = 3.40$, $\omega_p = 2\times10^{15}$ Hz, and $\gamma = 1.5\times10^{14}$ Hz respectively.[33] The RI of WS_2 is given in Ref. [12], which is $4.9 + 0.3124i$. The thickness of WS_2 is 0.8 nm.

Considering the reflection coefficient of p-polarized light, its expression is determined by the N-layer transfer matrix method.[35] The angular power distribution of the light is shown as follows:

$$dP \propto \frac{n_1^2 \sin\theta\cos\theta}{(1 - n_1^2\cos^2\theta)^2} d\theta. \tag{4}$$

Hence, when all guided light is emitted from the fiber, the

normalized transmit power of the fiber is determined by

$$P_{\text{trans}} = \frac{\int_{\theta_{\text{cr}}}^{\pi/2} R_{\text{P}}^{N_{\text{ref}}(\theta)} \dfrac{n_1^2 \sin\theta\cos\theta}{\left(1-n_1^2\cos^2\theta\right)^2}\,\mathrm{d}\theta}{\int_{\theta_{\text{cr}}}^{\pi/2} \dfrac{n_1^2 \sin\theta\cos\theta}{\left(1-n_1^2\cos^2\theta\right)^2}\,\mathrm{d}\theta}. \tag{5}$$

Here, $N_{\text{ref}}(\theta)$ and θ_{cr} are defined as $L/D\tan\theta$ and $\arcsin(n_{\text{cl}}/n_1)$, respectively: N_{ref} represents the total value of the reflections produced by the light and θ_{cr} is the critical angle when the fiber is totally reflected. And n_{cl} represents the RI of the cladding of the fiber.

For the SPR-based fiber optic biosensor with wavelength interrogation, when the RI of the sensing medium changes by δ_{ns}, the resonance wavelength changes by $\delta_{\lambda\text{res}}$, the sensitivity is defined as

$$S_n = \frac{\delta_{\lambda\text{res}}}{\delta_{\text{ns}}}. \tag{6}$$

Sensitivity is a standard parameter for evaluating the performance. That the resonance spectrum is deep and narrow means that the detection accuracy is high.

3. Results and discussion

The numerical simulations of the SPR-based optical fiber biosensor with Au/ZnO/WS_2 layer are studied in this paper. Not only is the MATLAB software used to analyze the SPR, but also COMSOL Multiphysics is applied to the optical SPR sensing model research. The analysis of the perspective of energy distribution provides a basis for the design and optimization.

The sensitivity of the structure of Au/ZnO/WS_2 is simulated by calculating the transmission output power of the sensor. In our work, the middle portion ($L = 15$ mm) of the multimode plastic clad silica fiber (numerical aperture NA = 0.24 and core diameter $D = 600$ μm) is selected to remove the cladding layer and then coated with Au/ZnO/WS_2 layer. This multilayer eventually contacts the sensing medium. The variation in RI of sensing medium will cause the resonance wavelength to change. The sensitivity is defined by Eq. (6). When the RI changes are the same, the sensitivity increases with wavelength drift increasing.

Figure 2 shows the transmission spectra of SPR biosensors with different coating materials: Au, Au/ZnO, and Au/ZnO/WS_2 (see Figs. 2(a)–2(c)). The thickness of the Au film is 40 nm and the thickness of ZnO is 5 nm. Figure 2(a) displays a transmission spectrum of conventional biosensor with only Au film, the resonance wavelength shift is about 58nm when the RI of the sensing medium is between 1.33 and 1.35. When a layer of ZnO is a coated Au film, the resonance wavelength shift is about 61 nm as shown in Fig. 2(b). As can be seen in Fig. 2(c), the wavelength shift of SPR sensor is 74 nm. It indicates that the sensor with the WS_2 sensing layer has a highest sensitivity.

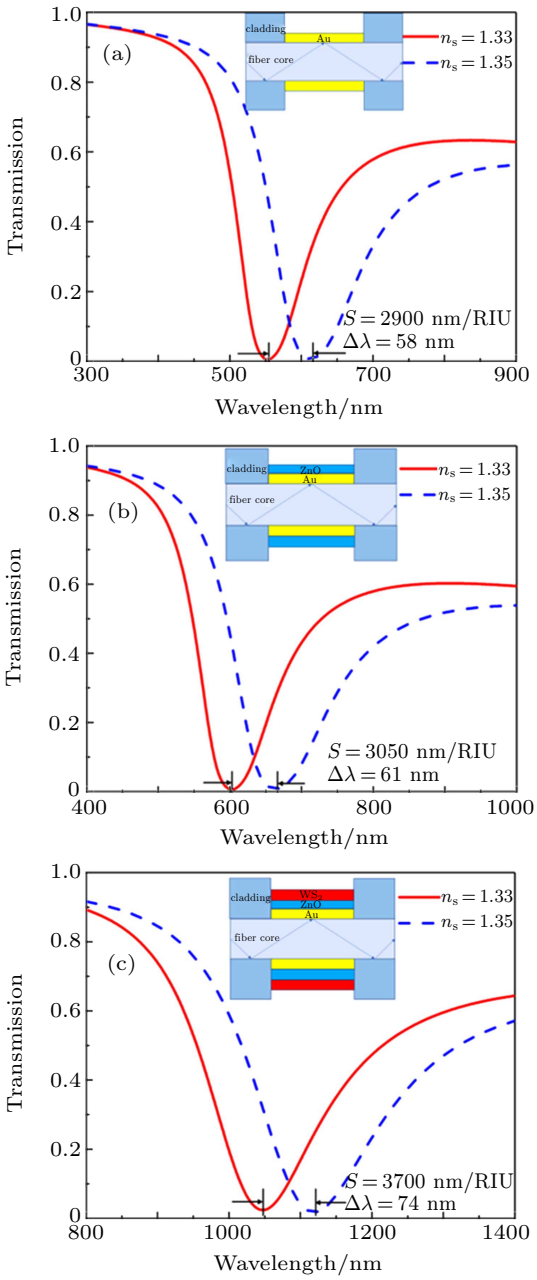


Fig. 2. Transmission spectra of SPR biosensors with different coating materials: (a) Au, (b) Au/ZnO, and (c) Au/ZnO/WS_2.

Next, the thickness values of the three layers of Au, ZnO, and WS_2 are optimized and then the sensor structure with higher sensitivity is designed theoretically. At first, the thickness of ZnO is tentatively to be 5 nm, WS_2 is of 2 layers and the RI of the sensing medium is set to be 1.33. By changing the thickness of the Au film (d_2) from 20 nm to 60 nm, the transmission spectra calculated theoretically are shown in Fig. 3. When the Au film is thin, the film thickness has a great influence on the position of the resonance peak and the full width at half maximum (FWHM). As the film thickness increases, the peak width narrows gradually. When the thickness exceeds 40 nm, the resonance peak becomes shallow. Also, the reso-

nance wavelength does not change significantly from 680 nm to 720 nm. The performance of the SPR sensor is evaluated in the quality of the formant. The ratio of depth of the resonance peak to FWHM is used to judge the formant. High-performance SPR sensors are more prone to choose structures with smaller FWHM and larger peak amplitudes. It is preferable to select 40 nm.

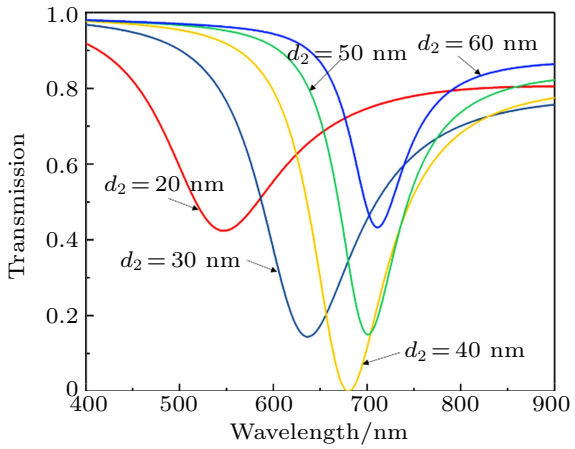


Fig. 3. Variations of tranmission with resonance wavelength for different values of Au film thickness.

After determining the thickness of Au film, thickness of ZnO layer and the number of layers of WS_2 are changed to optimize the structure. The resonance wavelengths of SPR fiber sensors with different thickness values of ZnO and WS_2 sensing layers are simulated. We calculate the sensitivity when the WS_2 changes from 2 layers to 18 layers with ZnO thickness being 5 nm, 10 nm, 15 nm, and 20 nm, respectively. The value of the sensitivity is the slope of the fitted line of the resonance wavelength *versus* RI of the SPR sensor. Figure 4(a) shows the transmittance *versus* wavelength curve for sensing structure of 40-nm Au/5-nm ZnO /14 layers WS_2 for the RI of the analyte varying from 1.33 to 1.37 (in steps of 0.01). In Fig. 4(b), the fitting relationships between the resonance wavelength of the SPR sensor with different WS_2 layers at different RI numbers are shown and the slope of the fitted line is the value of the sensitivity. With the increase of the number of WS_2 layers, it has an optimal value. The corresponding resonance wavelengths and the sensitivities of the fiber optic biosensor for different thickness values of ZnO and WS_2 are listed in Table 1. Obviously, the proposed SPR biosensor with 14 layers of WS_2 and 5-nm-thick ZnO has a highest sensitivity of 4310 nm/RIU. The sensor with Au/ZnO structure has been reported to have a sensitivity of 3161 nm/RIUin Ref. [33].

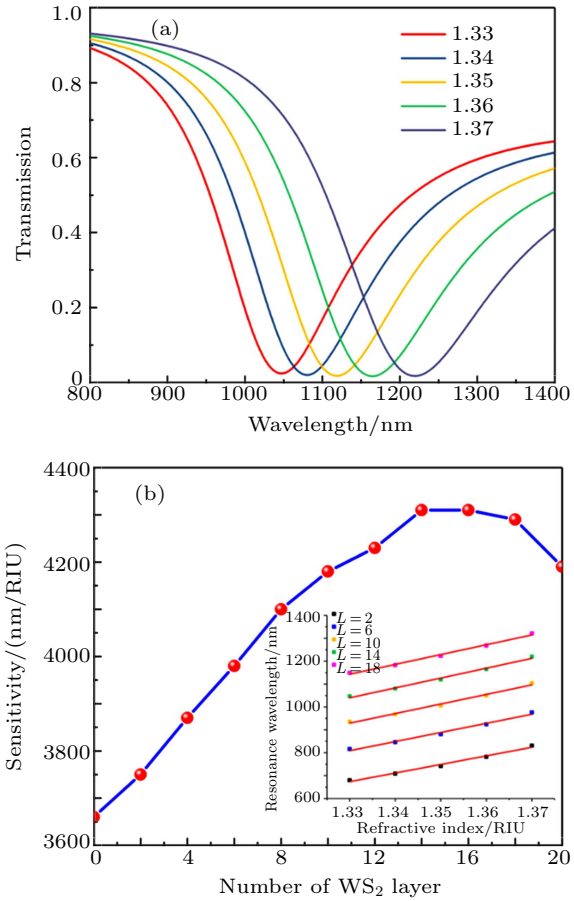


Fig. 4. (a) SPR transmission spectra of proposed fiber-optic biosensor at different RI values of the analyte, and (b) variation of sensitivity with the number of WS_2 layers, with inset showing the linear fits between the resonance wavelength and the RI of the analyte for various numbers of WS_2 sensing layers.

Table 1. Sensitivities of fiber-optic SPR biosensor with various thickness values of ZnO and WS_2.

Thickness of ZnO layer/nm	Sensitivity/(nm/RIU) Number of WS_2 layer								
	2	4	6	8	10	12	14	16	18
5	3750	3870	3980	4100	4180	4230	4310	4310	4290
10	3680	3710	3760	3760	3740	3680	3640	3600	3500
15	3560	3540	3490	3450	3340	3230	3150	3090	2970
20	3410	3340	3250	3160	3000	2860	2780	2720	2590

To further determine the method of improving the performance and explain the excitation of SPR, the electric field distribution of Au/ZnO/WS_2 structure is studied by COMSOL Multiphysics. For verifying that WS_2 enhances surface plasmon resonance, the finite element simulations of the traditional Au structure, Au/ZnO structure and Au/ZnO/WS_2 structure are conducted, respectively. When the structure is of 40-nm Au/5-nm ZnO/14 layers of WS_2, the electric field intensity

distribution of the TM polarization is described in Fig. 5(a) with RI fixed at 1.33. It can be found that the electric field is locally enhanced compared with the case for the sensors of conventional construction due to the presence of ZnO and WS_2 layers. A enlarged view for part of the electric field distribution of the structure is shown. When the SPR phenomenon occurs near the Au film, the electric field is enhanced again on the surface of WS_2. The surface plasmon waves propagate along the interface because of the combination of the SPR phenomenon and the guided-wave surface-plasmon-resonance configuration. Due to the high refractive index material (ZnO and WS_2), the sensitivity is increased by increasing the transmission depth of the evanescent wave.

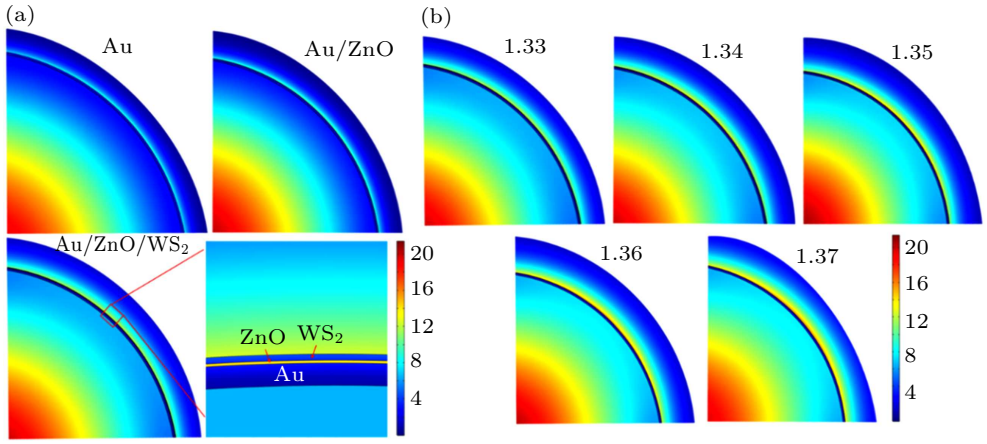


Fig. 5. (a) Mode field distribution of Au, Au/ZnO, and proposed Au/ZnO/WS_2 SPR biosensor at sensing medium RI of 1.33, respectively, and (b) mode field distribution of proposed biosensor at the analyte RI from1.33 to 1.37 (in steps of 0.01), respectively.

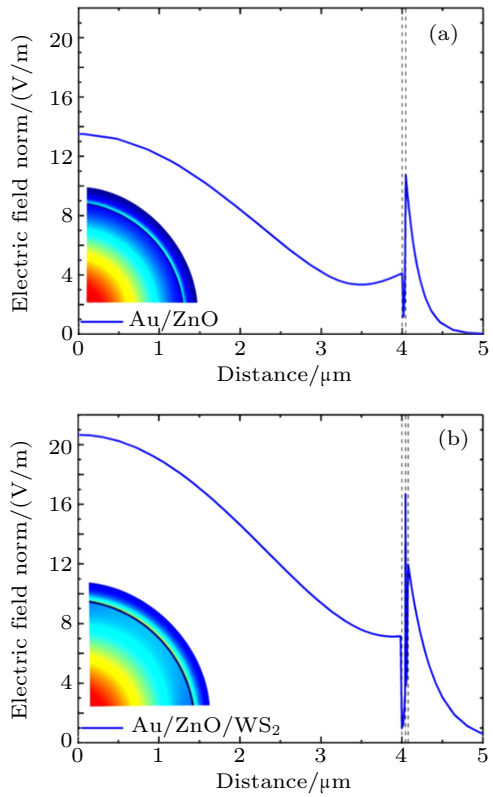


Fig. 6. Comparison of normalized electric field *versus* distance curve between (a) SPR sensor with Au/ZnO structure and (b) that with Au/ZnO/WS_2 structure.

Figure 5(b) shows the electric field distributions of SPR mode of the biosensor with Au/ZnO/WS_2 structure having different RI numbers of the sensing medium. With the increase of the analyte RI number, the guided mode inside the fiber becomes weaker and the electric field intensity is stronger on the surface of the Au film. With the RI of the analyte varying from 1.33 to 1.37, the effective RI value of the SPR mode increases and the resonance wavelength shifts toward the long wave. When resonance occurs, the surface of metal medium will couple more energy, which enhances the resonance intensity. Therefore, the electric field near the metal is enhanced. It clearly shows that a little change in RI of sensing medium will lead to a dramatic change in the characteristics of surface wave.

Furthermore, figure 6 shows the normalized electric field direction diagram of the radial energy distribution of the SPR biosensor with Au/ZnO and that with Au/ZnO/WS_2. As shown in Fig. 6(a), the Au layer can enhance the electric field intensity and present a peak value at the surface of Au film, which means the excitation of SPR. In Fig. 6(b), the presence of WS_2 layer reinforces the electric field again, resulting in the enhancement of SPR excitation because of the high mobility of electrons.

In addition, WS_2 with the pore-like structure shortens the electron transport distance of the active center of the surface, thereny improving the ability to transport electrons. Also, it is significant to mention here that Au/ZnO nanostructure has good optical response[36,37] and ZnO-WS_2 heterostructure has good photoresponsivity and excellent photocatalytic activity.[38] This structure can increase the carrier mobility of WS_2 and the photocarrier transport which contributes to the enhancement of SPR and then improves the performance. Ta-

ble 2 shows the comparison of performance between our proposed Au/ZnO/WS_2-coated SPR sensor and other sensors reported in the literature.

Table 2. Comparison of performance between proposed sensor and other sensors.

Structure	RI range	Sensitivity/(nm/RIU)	Reference
Ag/graphene	1.46–1.49	300	[40]
Au/ZnO	1.30–1.37	3161	[33]
Au/TiO_2	1.333–1.403	1015.15	[41]
Au/WS_2	1.333–1.360	2459.3	[30]
Au/ZnO/WS_2	1.33–1.37	4310	this work

The simulation results of Au/ZnO/WS_2 structure SPR optical fiber sensor for measuring the concentration of glucose are discussed. In Ref. [39] the relationship between average refractive index and glucose concentration was studied. The linear relationship is represented by the following linear expression:

$$n_{g/l} = 0.00011889C + 1.33230545, \tag{7}$$

where C represents the glucose concentration (in units g/l) and $n_{g/l}$ denotes the average refractive index.

Since the SPR absorption peak is related to the RI of the solution, the change in RI of the glucose solution can be measured. When obtaining the position of the SPR formant, RI of the solution can be known and it can be in one-to-one correspondence to the glucose concentration. The correspondences among the glucose concentration, the refractive index and the resonance wavelength of two structures are shown in Table 3.

Table 3. Correspondence among glucose concentration, refractive index, and resonance wavelength.

Glucose concentration/(g/l)	Refraction index/(RIU)	Resonance wavelength/nm	
		Au/ZnO	Au/ZnO/WS_2
	1.33	603	1047
65	1.34	631	1080
149	1.35	664	1119
233	1.36	703	1165
317	1.37	750	1220

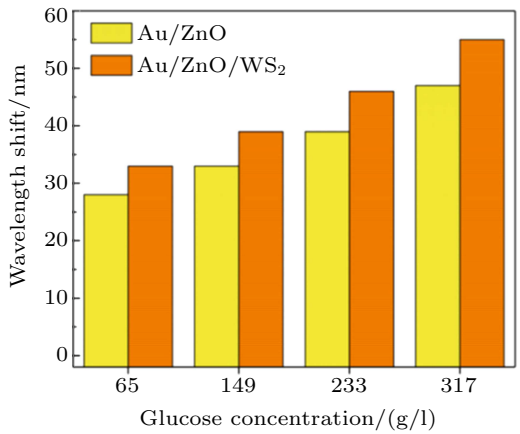


Fig. 7. Comparison of measurement of glucose concentration between two structures.

The sensitivity of the biosensor is proportional to the degree of the drift of the resonance wavelength. As shown in Fig. 7, the wavelength red-shift increases significantly in the structure of the proposed. Applying this theory to practice, we may find that the sensitivity and accuracy of measuring glucose concentration can both be improved.

4. Conclusions

In this paper, an SPR-based optical fiber biosensor with Au/ZnO/WS_2 structure for detecting glucose concentration is proposed and analyzed theoretically. It is verified that the addition of WS_2 can significantly enhance the sensitivity. For glucose concentration detection, WS_2 material has advantages of strong adsorption capacity for GOx. By analyzing resonance wavelength, the RI of the solution can be calculated. The glucose concentration can be obtained by the correspondence between RI and glucose concentration. The highest enhanced sensitivity of SPR-based optical fiber biosensor is achieved at 4310 nm/RIU with the structure of 40-nm Au/5-nm ZnO/14 layers of WS_2. The proposed WS_2-based SPR fiber biosensor has a unique effect on the detection of glucose concentration. It is expected to have potential applications in future medical blood glucose concentration detection.

References

[1] Asif M H, Ali S M U, Nur O, Willander M, Brännmark C, Strålfors P, Englund U H, Elinder F and Danielsson B 2010 *Biosens. Bioelectron.* **25** 2205
[2] Iwasaki Y, Horiuchi T and Niwa O 2001 *Anal. Chem.* **73** 1595
[3] Singh S and Gupta B D 2013 *Sens. Actuators B: Chem.* **177** 589
[4] Sharma A K and Gupta B D 2007 *J. Appl. Phys.* **101** 093111
[5] Wu L, Chu H S, Koh W S and Li E P 2010 *Opt. Express* **18** 14395
[6] Homola J 1995 *Sens. Actuators B: Chem.* **29** 401
[7] Lin W B, Jaffrezic-Renault N, Gagnaire A and Gagnaire H 2000 *Sens. Actuators A: Phys.* **84** 198
[8] Sharma A K and Gupta B D 2004 *Sens. Actuators B: Chem.* **100** 423
[9] Lee K L, Lee C W, Wang W S and Wei P K 2007 *J. Bio. Opt.* **12** 044023
[10] He L, Musick M D, Nicewarner S R, Salinas F G, Benkovic S J, Natan M J and Keating C D 2000 *J. Am. Chem. Soc.* **122** 9071
[11] Zhao J, Zhang X, Yonzon C R, Haes A J and Van Duyne R P 2006 *Nanomedicine* **1** 219
[12] Wu L, Guo J, Wang Q, Lu S, Dai X, Xiang Y and Fan D 2017 *Sens. Actuators B: Chem.* **249** 542
[13] Lahav A, Auslender M and Abdulhalim I 2008 *Opt. Lett.* **33** 2539
[14] Shalabney A and Abdulhalim I 2011 *Laser Photon. Rev.* **5** 571
[15] Homola J 2003 *Anal. Bioanal. Chem.* **377** 528
[16] Meshginqalam B, Ahmadi M T, Ismail R and Sabatyan A 2017 *Plasmon.* **12** 1991
[17] Zeng S, Baillargeat D, Ho H P and Yong K T 2014 *Chem. Soc. Rev.* **43** 3426
[18] Xu M, Liang T, Shi M and Chen H 2013 *Chem. Rev.* **113** 3766
[19] Eda G and Maier S A 2013 *ACS Nano* **7** 5660
[20] Bagdžiūnas G and Ramanavičius A 2019 *Phys. Chem. Chem. Phys.* **21** 2968
[21] Li W, Ding C, Cai Y, Liu J, Wang L, Ren Q and Xu J 2018 *Sensors* **18** 660
[22] Li W, Dai E, Bai G and Xu J 2016 *Sens. Actuators B: Chem.* **237** 526
[23] Li W, Hu M, Ge P, Wang J and Guo Y 2014 *Appl. Surf. Sci.* **317** 970
[24] Ouyang Q, Zeng S, Jiang L, Hong L, Xu G, Dinh X Q, Qian J, He S, Qu J, Coquet P and Yong K T 2016 *Sci. Rep.* **6** 28190

[25] Pandey P, Singh S P, Arya S K, Gupta V, Datta M, Singh S and Malhotra B D 2007 *Langmuir.* **23** 3333
[26] Shan C, Yang H, Song J, Han D, Ivaska A and Niu L 2009 *Anal. Chem.* **81** 2378
[27] Zhang H, Meng Z, Wang Q and Zheng J 2011 *Sens. Actuators B: Chem.* **158** 23
[28] Usha S P, Shrivastav A M and Gupta B D 2016 *Biosens. Bioelectron.* **85** 986
[29] Luo Y, Chen C, Xia K, Peng S, Guan H, Tang J, Lu H, Yu J, Zhang J, Xiao Y and Chen Z 2016 *Opt. Express* **24** 8956
[30] Wang H, Zhang H, Dong J, Hu S, Zhu W, Qiu W, Lu H, Yu J, Guan H, Gao S, Li Z, Liu W, He M, Zhang J, Chen Z and Luo Y 2018 *Photon. Res.* **6** 485
[31] Zhu S, Gong L, Xie J, Gu Z and Zhao Y 2017 *Small Methods* **1** 1700220
[32] Sharma A K and Gupta B D 2005 *Opt. Commun.* **245** 159
[33] Shukla S, Sharma N K and Sajal V 2015 *Sens. Actuators B: Chem.* **206** 463
[34] Ordal M A, Long L L, Bell R J, Bell S E, Bell R R, Alexander R W and Ward C A 1983 *Appl. Opt.* **22** 1099
[35] Mishra A K, Mishra S K and Gupta B D 2015 *Opt. Commun.* **344** 86
[36] Balevicius Z, Paulauskas A, Plikusiene I, Mikoliunaite L, Bechelany M and Popov A 2018 *J. Mater. Chem. C* **6** 8778
[37] Viter R, Balevicius Z, Chaaya A A, Baleviciute I, Tumenas S, Mikoliunaite L, Ramanavicius A, Gertnere Z, Zalesska A, Vataman V, Smyntyna V, Erts D, Miele P and Bechelany M 2015 *J. Mater. Chem. C* **3** 6815
[38] Lan C, Li C, Wang S, Yin Y, Guo H, Liu N and Liu Y 2016 *RSC Adv.* **6** 67520
[39] Yeh Y L 2008 *Opt. Lasers Eng.* **46** 666
[40] Rifat A A, Mahdiraji G A, Chow D M, Shee Y G, Ahmed R and Adikan F R M 2015 *Sensors* **15** 11499
[41] Liu K, Xue M, Jiang J, Wang T, Chang P and Liu T 2018 *Opt. Commun.* **410** 552